

## Microscopic Structure of Er-Related Optically Active Centers in Si

H. Przybylinska<sup>1</sup>, N. Q. Vinh<sup>2</sup>, B.A. Andreev<sup>3</sup>, Z. F. Krasil'nik<sup>3</sup>, and T. Gregorkiewicz<sup>2</sup>

<sup>1</sup>Institute of Physics, Polish Academy of Sciences,  
Al. Lotników 32/46, PL-02 668 Warsaw, Poland

<sup>2</sup>Van der Waals–Zeeman Institute, University of Amsterdam,  
Valckenierstraat 65, NL-1018 XE Amsterdam, The Netherlands

<sup>3</sup>Institute for Physics of Microstructures, GSP-105, 603600 Nizhny Novgorod, Russia

### ABSTRACT

A successful observation and analysis of the Zeeman effect on the near 1.54  $\mu\text{m}$  photoluminescence spectrum in Er-doped crystalline MBE-grown silicon are reported. A clearly resolved splitting of 5 major spectral components was observed in magnetic fields up to 5.5 T. Based on the analysis of the data the symmetry of the dominant optically active center was conclusively established as orthorhombic I ( $C_{2v}$ ), with  $g_{\parallel} \approx 18.4$  and  $g_{\perp} \approx 0$  in the ground state. The fact that  $g_{\perp} \approx 0$  explains why EPR detection of Er-related optically active centers in silicon may be difficult. Preferential generation of a single type of an optically active Er-related center in MBE growth confirmed in this study is essential for photonic applications of Si:Er.

### INTRODUCTION

The trivalent erbium ion gives rise to the characteristic emission near 1.54  $\mu\text{m}$ , due to the  $^4I_{13/2} \rightarrow ^4I_{15/2}$  transition, which is practically independent of the host material. Since this particular wavelength coincides with the absorption minimum of silica glass fibres used for telecommunication networks, erbium doping of semiconductors has attracted considerable attention, in particular, the technologically important Si:Er system. As a result of a continued research effort Si:Er-based devices, such as optical amplifiers and light emitting diodes have been successfully developed (for an up-to-date review see, e.g. [1]). Despite that, many of the more fundamental aspects of the Si:Er system, such as the microscopic structure of the optically active Er centers in silicon or the relevant energy transfer mechanisms [2], remain controversial.

In Er implanted silicon numerous attempts have been made to identify the location, site symmetry and nearest neighbors of the Er impurity. In EXAFS experiments [3,4] either silicide like or oxide like surrounding of the Er impurity was observed, depending on the oxygen content and thermal annealing conditions. In channeling experiments, on the other hand, Er at the tetrahedral interstitial lattice site was found to be the dominant center [5], in agreement with theoretical predictions [6]. In EPR several low symmetry Er-O complexes were identified, none of them related to the centers dominant in photoluminescence (PL) [7]. Apparently, the concentration of optically active centers in Er-implanted Si is too low to be detected otherwise than optically. Microscopic information on the Er-related emitting centers would be best obtained in a magneto-optical study. However, due to the great multiplicity of centers formed in crystalline silicon by Er implantation [8], with often overlapping PL spectra no observation of the Zeeman effect in PL has been so far possible.

The situation is different in Er doped silicon grown by sublimation MBE, where a preferential formation of a single type of center, labeled Er-1, has been observed [9]. The

extremely narrow linewidth ( $<10 \mu\text{eV}$ ) made a successful observation of the Zeeman effect on the  $\text{Er}^{3+}$  related photoluminescence possible [10].

## EXPERIMENTAL DETAILS

The sample was grown by sublimation molecular beam epitaxy on (100) Si substrate and consisted of 400 interchanged Si and Si:Er layers of 1.7 nm and 2.3 nm thickness, respectively, stacked along the  $\langle 100 \rangle$  growth direction.

The experiments were performed at liquid helium temperature using the 514.5 nm Ar-ion laser line for excitation. The sample was placed in a split-coil superconducting magnet with optical access. The photoluminescence was dispersed through a high-resolution 1.5 m  $f/12$  monochromator (Jobin Yvon THR-1500) equipped with a 600 grooves/mm grating blazed at  $1.5 \mu\text{m}$ , and detected with a liquid-nitrogen cooled Ge detector (Edinburgh Instruments). For polarization measurements a quarter-lambda plate and a linear polarization filter were used. The experimental configuration permitted observation of the luminescence along and perpendicular to the field direction.

## RESULTS AND DISCUSSION

The photoluminescence (PL) measurements of the Si/Si:Er superlattice reveal an intense spectrum, shown in Fig. 1, consisting of only a few narrow lines (the width of the most intense line is less than  $0.1 \text{ cm}^{-1}$ ). This spectrum was assigned to a single type of center, labeled Er-1, of noncubic symmetry [9].

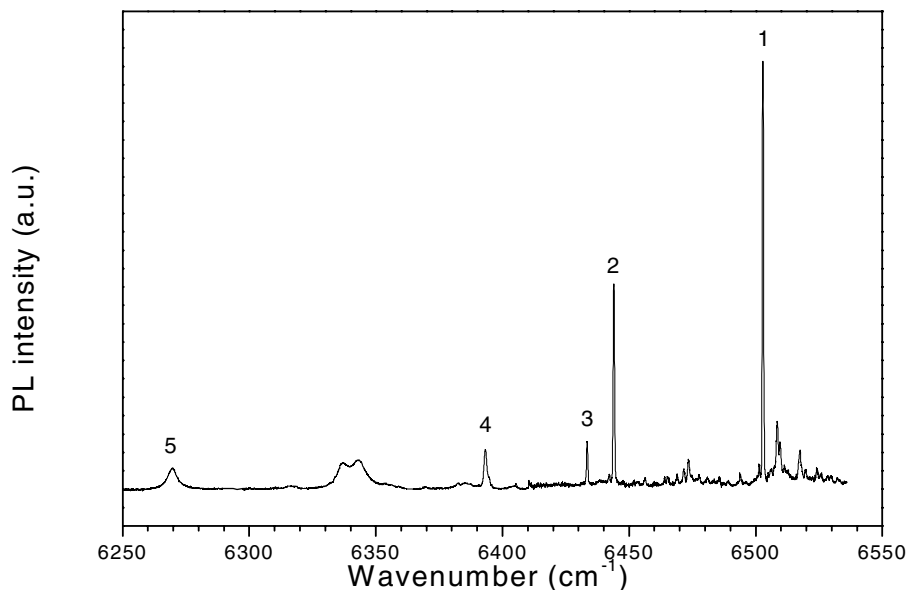


**Figure 1.** Photoluminescence spectrum of the multilayer Si/Si:Er structure measured at 4.2. The numbers mark the emission lines for which the Zeeman effect was investigated.

In a crystalline environment of lower than cubic symmetry the excited  $^4I_{13/2}$  and ground  $^4I_{15/2}$  states of  $\text{Er}^{3+}$  split into 7 and 8 Kramers doublets, respectively. At low temperatures only transitions from the lowest  $^4I_{13/2}$  doublet will be observed, resulting in 8 PL lines, each corresponding to transitions between effective spin doublets. In an external magnetic field the degeneracy of the doublets will be lifted due to the Zeeman effect and the PL lines will split into components in a pattern reflecting the site symmetry of the  $\text{Er}^{3+}$  center. The Hamiltonian describing the Zeeman splitting is given by:

$$H = \mu_B \mathbf{B} \cdot \mathbf{g} \cdot \mathbf{S} \quad (1)$$

where  $\mu_B$  is the Bohr magneton,  $\mathbf{g}$  the effective g-tensor, and  $S=1/2$  is the effective spin. In general, every PL line will split into four components, with  $\Delta h\nu = \pm 1/2 |g' - g| \mu_B B$  for  $\Delta M_S = 0$  transitions and  $\Delta h\nu = \pm 1/2 |g' + g| \mu_B B$  for  $\Delta M_S = \pm 1$  transitions, where  $g'$  and  $g$  are the effective g values of the upper and lower doublets, respectively. However, the magnetic dipole allowed  $\Delta M_S = \pm 1$  transitions have low probability and for the Er ion usually only transitions without spin flip are observed.

This is also the case for the Er center investigated in this study. None of the emission components appearing upon application of magnetic field was found to possess a measurable degree of circular polarization, which means that only splitting with the effective g-value of  $|g' - g|$  occur. Though  $g'$  and  $g$  may be quite large, their difference will be small (unless one of the g-

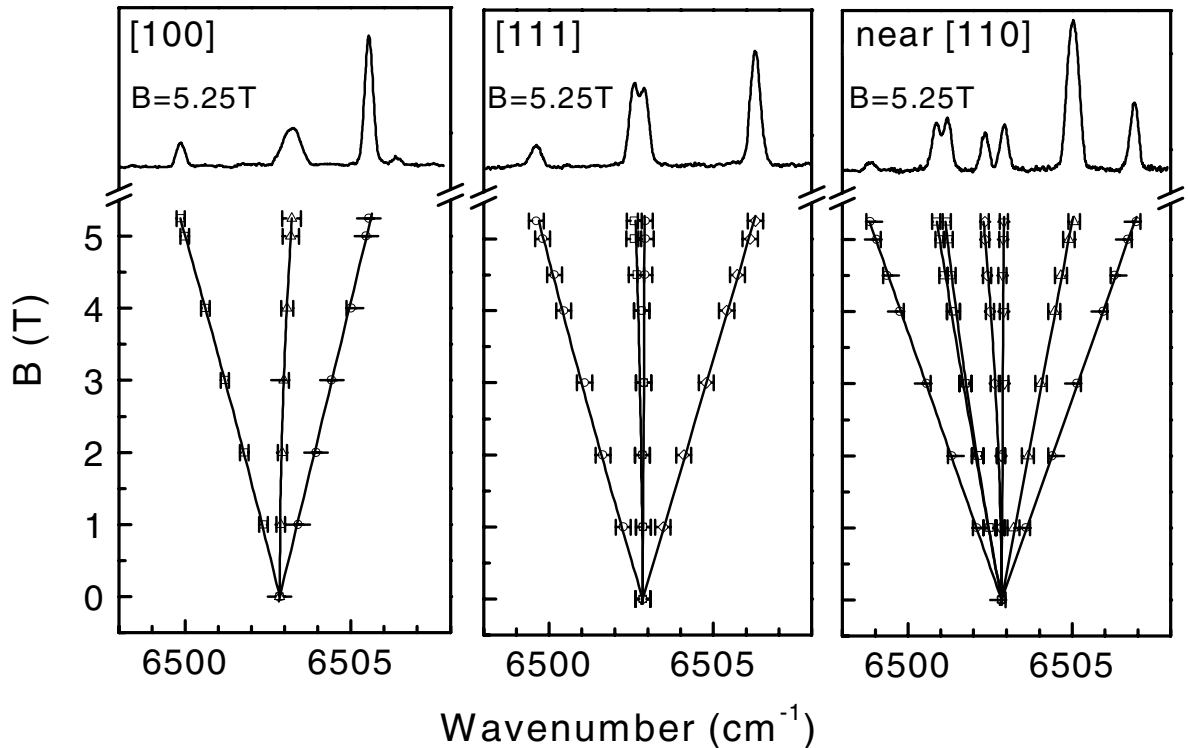


**Figure 2.** Magnetic field induced splitting of the main PL line (labeled 1 in Fig.1) at 4.2 K for  $\mathbf{B}$  oriented along the [100], [111], and near [110] crystallographic axes. The "error bars" give the full width at half maximum of the Zeeman split components.

factors is negative) and rather high magnetic fields have to be applied in order to observe a well resolved splitting. In consequence, the magnitude of the Zeeman splitting becomes comparable to the crystal field splitting and mixing between the individual sublevels in the  $J=15/2$  and  $J=13/2$  manifolds is expected. In the particular case of the dominant PL line (labeled 1 in Fig.1), only transitions from lower lying level of the excited state doublet to the lower lying level of the ground state doublet will be unaffected for an arbitrary direction of the magnetic field, since these are not disturbed by the proximity of other Er-related levels. In contrast, other Zeeman components will show higher order contributions in  $B$ . The former transitions are easily identified since their intensity is higher due to partial thermalization.

Figure 2 shows the Zeeman effect for the PL line labeled 1. In magnetic fields of up to 5.25 T, the splitting into three components for  $\mathbf{B}||[100]$ , four components for  $\mathbf{B}||[111]$ , and seven components for  $\mathbf{B}$  near  $[110]$  can be observed. Note that the position of the central component is nearly independent of  $B$  for all three field orientations. In fact, the small splitting resolved at high fields for the  $[111]$  and  $[110]$  directions, as well as the linewidth broadening observed for  $\mathbf{B}||[100]$  are almost entirely due to second order effects and depend quadratically on  $B$ . For this Zeeman component the effective  $g$  factors of the upper and lower states must be almost equal. It can be also seen that the more intense lines, related to transitions from the lower Zeeman level of the excited state doublet occur at higher energies, which thus gives us the additional information that for those lines  $|g'| < |g|$ .

Keeping the magnetic field fixed at 5.25 T and rotating its direction, we observe a

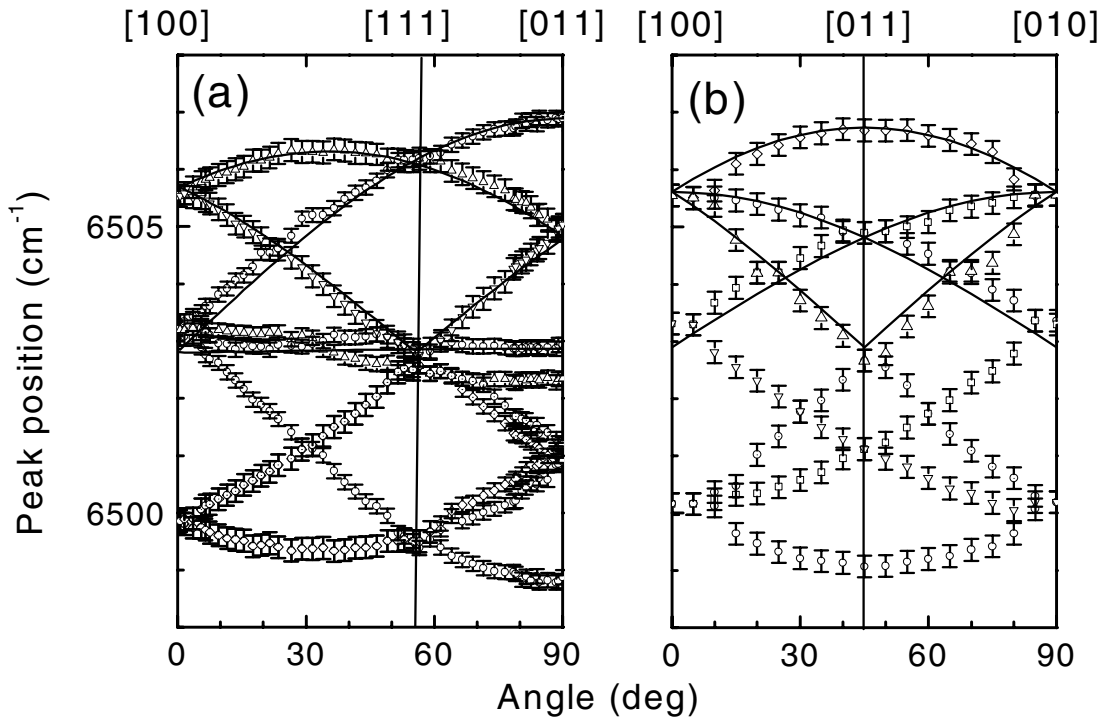


**Figure 3.** Angular dependence of the Zeeman splitting of the main PL line (labeled "1" in Fig. 1) at 5.25 T for the magnetic field rotated in the (011) (a) and (100) (b) crystallographic planes. Solid lines correspond to simulations with the  $g$ -values given in the text, without taking into account second order corrections.

pronounced angular dependence of the line positions indicative of a center with lower than cubic site symmetry. Figure 3 shows the positions of PL lines for the magnetic field rotated in the (011) and (100) planes. As can be seen, the center has four nonequivalent orientations for an arbitrary direction of  $\mathbf{B}$  in both planes. Although the angular dependence is complicated by anticrossings among the sublevels, it can be clearly concluded that the center possesses orthorhombic I ( $C_{2v}$ ) site symmetry.

The data presented in Fig. 3(b) show, moreover, that the superlattice stacking direction has no measurable influence upon the symmetry of the Er-related optically active center. In this angular dependence the magnetic field direction was rotated from the  $\langle 100 \rangle$  growth direction, perpendicular to the sample surface, to an equivalent  $\langle 100 \rangle$  direction within the plane of the sample. As can be seen, the observed pattern is fully symmetric.

For a  $C_{2v}$  symmetry center, two of the main tensor axes are oriented along two perpendicular  $\langle 011 \rangle$  directions, in group theory taken as  $x$  and  $y$  axes, while the  $z$  axis is the  $\langle 100 \rangle$  oriented intersection of the planes perpendicular to  $x$  and  $y$ . In this paper we choose the spin quantization axis,  $z$ , along the tensor principal axis with the greatest  $g$  value, which in this case is one of the  $\langle 110 \rangle$  directions. The principal values of the effective  $g$  tensor  $\mathbf{g}_{\text{eff}} = |\mathbf{g}' - \mathbf{g}|$  can be determined from the Zeeman splitting shown in Fig. 2. We obtain:  $\Delta g_z = |g_z - g_z'| = 3.29 \pm 0.03$ ,  $\Delta g_x \cong \Delta g_y \cong 0$ , and  $g_x' \cong g_y' \cong g_x \cong g_y \cong 0$ , within the experimental error. As can be seen from the solid lines in Fig. 3, simulation with the Hamiltonian (1) gives a satisfactory agreement with the experimental data, despite neglecting second order effects.

For obvious reasons the individual  $z$  components of the  $g$  tensors of the upper and lower doublets cannot be determined based on the results of the experiments discussed so far. However,  $g_z'$  can be estimated from the intensity ratio of the low and high energy components, which at

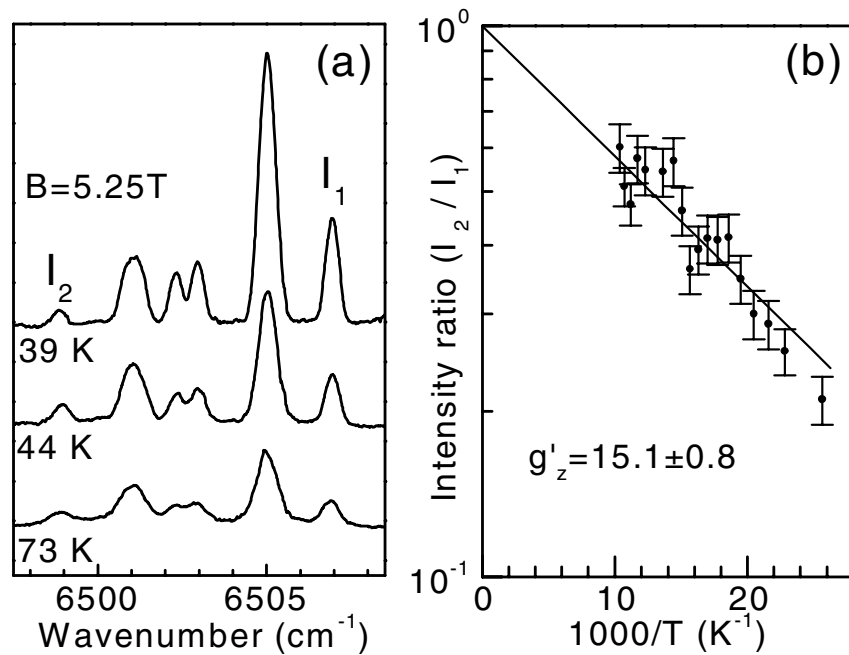


**Figure 4.** (a) Magnetic field induced splitting of the main PL line at 5.25 T and temperatures indicated in the figure for  $\mathbf{B} \parallel [011]$ . (b) The intensity ratio  $I_2/I_1$  fitted assuming thermalization within the upper doublet.

temperatures high enough to ensure Boltzmann distribution reflects the actual Zeeman splitting of the excited state. The PL spectra for the magnetic field oriented along the [001] direction at 5.25 T and three different temperatures are shown in Fig. 4. As can be seen, the intensity ratio of the PL components labeled  $I_2$  and  $I_1$  allows us to estimate  $g_z'$  as  $15.1 \pm 0.8$ . This gives us the  $g_z$  value for the ground state doublet of  $18.4 \pm 0.81$ . Note that the two components related to  $\Delta g_y$  (the central lines in Fig. 4) have equal intensities independent of the temperature, consistent with  $g_y' \cong 0$ .

We are dealing with a particular situation where  $g_{\perp}$  is close to zero for both the ground and the excited state doublets. The fact that  $g_{\perp} \cong 0$  implies a low probability of spin transitions within the ground state and explains why the Er-related optically active center in crystalline silicon has not been detected using magnetic resonance. The  $g$  tensor for the ground state doublet ( $g_{\parallel} \cong 18.4$  and  $g_{\perp} \cong 0$ ) results in a trace of 18.4. In the presence of small distortions to tetrahedral symmetry the average  $g_{av}$  factor would relate to the isotropic cubic  $g_c$  factor in the following way:  $g_{av} = g_c = \frac{1}{3}(g_{\parallel} + 2g_{\perp})$  [11]. Here  $g_{av} = 6.13 \pm 0.5$ , which is similar to the values found for Er in different host materials [7,12,13]. In  $T_d$  symmetry the  $g$  factors of  $\Gamma_6$  and  $\Gamma_7$  doublets are +6.8 and -6.0, respectively [11]. It seems, therefore, that in the present case the ground state is more likely to have a  $\Gamma_6$  character which, together with the PL line pattern remarkably resembling that of the tetrahedral interstitial PL center observed in Er-implanted silicon [7,8], would imply interstitial location. However, the  $C_{2v}$  distortion is too strong to be considered as a small perturbation, which makes the above approach invalid. Still, in recent total energy calculations the  $T_d$  interstitial site with  $C_{2v}$  distortion was considered as the most stable configuration of the  $Er^{3+}$  ion in crystalline silicon [14].

## CONCLUSIONS

We have provided direct microscopic information on the structure of a prominent center responsible for optical activity of Er in crystalline silicon. From a clear Zeeman effect observed on the main line of the Er-1 PL spectrum, the lower than cubic symmetry of the emitting center is confirmed and conclusively identified as orthorhombic I ( $C_{2v}$ ) with  $g$  tensor of the ground state  $g_{\parallel} \cong 18.4$  and  $g_{\perp} \cong 0$ . We note that the preferential formation of one type of Er-related optically active center, as confirmed by the success of the reported Zeeman effect study, is a necessary prerequisite for development of efficient photonic devices based on Si:Er.

## REFERENCES

1. S. Coffa *et al.*, Mater. Res. Bull. **23**, 25 (1998).
2. J. Palm *et al.*, Phys. Rev. B **54**, 17603 (1996).
3. D. L. Adler *et al.*, Appl. Phys. Lett. **61**, 2181 (1992).
4. A. Terrasi *et al.*, Appl. Phys. Lett. **70**, 1712 (1997)
5. U. Wahl *et al.*, Phys. Rev. Lett. **79**, 2069 (1997).
6. M. Needels *et al.*, Phys. Rev. B **47**, 15 533 (1993).
7. J. D. Carey *et al.*, Phys. Rev. B **59**, 2773 (1999).
8. H. Przybylinska *et al.*, Phys. Rev. B **54**, 2532 (1996).

9. B. A. Andreev *et al.*, J. Cryst. Growth **201/202**, 534 (1999); M.V. Stepikhova *et al.*, Thin Solid Films **369**, 426 (2000).
10. N.Q. Vinh *et al.*, Phys. Rev. Lett. **90**, 66401 (2003)
11. A. Abragam and B. Bleaney, *Electron Paramagnetic Resonance of Transition Metal Ions*, Clarendon Press, Oxford 1970
12. R. K.Watts and W.C. Holton, Phys. Rev. **173**, 417 (1968).
13. J. D. Kingsley and M. Aven, Phys. Rev. **155**, 235 (1967).
14. A.G. Raffa and P. Ballone, Phys. Rev. B **65**, 121309 (2002).

## ACKNOWLEDGEMENTS

The work was financially supported by the *Nederlandse Organisatie voor Wetenschappelijk Onderzoek* (NWO), the *European Research Office* (ERO), and State Committee of Scientific Research (KBN) project No. PB 1596/T11/2001/21.